*Free Rad. Res.*, Vol. 20, No. 2, pp. 71-82
Reprints available directly from the publisher
Photocopying permitted by license only



# RADICAL INTERMEDIATES IN THE REDOX REACTIONS OF TETRAZOLIUM SALTS IN APROTIC SOLVENTS
## (Cyclovoltammetric, EPR and UV-VIS study)

PETER RAPTA, VLASTA BREZOVÁ, MICHAL ČEPPAN, MILAN MELNIK, DUŠAN BUSTIN, ANDREJ STAŠKO*

*Faculty of Chemistry, Slovak Technical University, SK-812 37 Bratislava, Slovakia*

*(Received May 5th, 1993; in revised form September 19th, 1993)*

Tetrazolium Blue ($TBCl_2$) and Nitrotetrazolium Blue ($NTBCl_2$) cathodically reduced in non aqueous solvents form radicals with the center of unpaired electron on the tetrazolyl ring (TBH·, NTBH·) as detected by EPR spectroscopy. After prolonged reduction, formazans ($TBH_2$, $NTBH_2$) are formed and are then further reduced to the nitro-centered anion radical (from $NTBH_2$) and the azogroup-centered anion radical (from $TBH_2$). The first cathodic peak in the cyclovoltammetric study in the region from −0.3 to −0.6 V vs. SCE (saturated calomel electrode) is irreversible and indicates an adsorption and diffusion process on the platinum and mercury electrodes. Formation of $TBH^+$ and $NTBH^+$ is assumed. The second peak, in the region from −0.8 to −1.3 V vs. SCE, is nearly reversible and coupled with the formation of TBH· and NTBH· radicals. UV-VIS spectra measured during the reduction show isosbestic points at the conversions: $TB^{++} \rightarrow TBH^+$, $NTB^{++} \rightarrow NTBH^+$; further, $TBH^+ \rightarrow TBH_2$ and $NTBH^+ \rightarrow NTBH_2$. The characteristic colours of the solutions observed can be used to characterise the reduction state of tetrazolium salts.



## INTRODUCTION

Tetrazolium salts as electron acceptors are widely used as redox indicators in histochemistry, pharmacology and in various biochemical applications. Thus Nitrotetrazolium Blue ($NTBCl_2$) is frequently used to identify superoxide in biochemical systems[1] as it forms coloured products. In spite of all these broad applications, relatively little attention has been paid to the mechanism and radical intermediates in their redox reactions. Therefore, we investigated their electrochemical behavior in aprotic solvents. Current investigations in aqueous solutions indicate a shift of cathodic potentials with pH[2,3] and an integral four electron reduction step.[4] This reduction[5,6] was described by two irreversible two-electron steps and characterised in the following reaction scheme:

$$TB^{2+} + 2e^- + H^+ \rightarrow TBH^+ \text{ (solution, adsorbed)}$$

$$TBH^+ + 2e^- + H^+ \rightarrow TBH_2 \text{ (solution, adsorbed)}$$

The first and the second steps include diffusion and adsorption processes. The formation of radical intermediates $TB^{+\cdot}$ and $TBH^{+\cdot}$ is assumed, but not yet confirmed by EPR. Simultaneously, UV-VIS spectra indicated two reduction products of tetrazolium salts.[6-8] By the stopped-flow method and pulse radiolysis $NTB^{+\cdot}$ radical was assumed from UV-VIS investigation.[9] In the case of

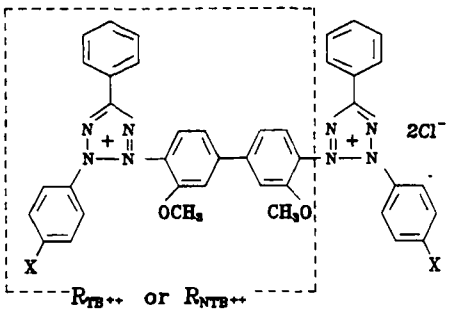


$TB^{++}$ if X is H

$NTB^{++}$ if X is $NO_2$

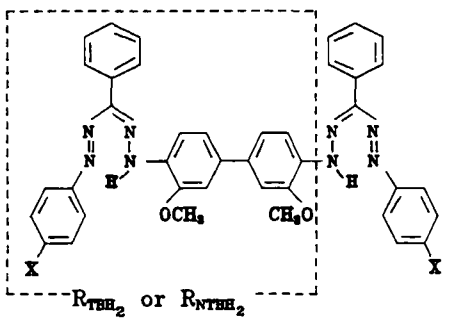


$TBH_2$ if X is H

$NTBH_2$ if X is $NO_2$

FIGURE 1 Formulae and abbreviations of Tetrazolium blue ($TBCl_2$) and Nitrotetrazolium Blue ($NTBCl_2$).

2,3,5-triphenyl tetrazolyl,[10] a tetrazolyl centered radical was observed in EPR. The proton hyperfine interactions on the phenyl ring[11], the influence of its substituents on the distribution of unpaired electron[12] and the formation of bis-formazans[13] were studied in aprotic media. In this paper, the electrochemical investigations carried out in aqueous solution were expanded to aprotic solvents acetonitrile, dimethylformamide, dimethylsulfoxide and dichloromethane. In cathodic reduction, the radical intermediates were generated, identified and characterised by means of EPR and UV-VIS techniques.

## EXPERIMENTAL

Tetrazolium blue ($TBCl_2$) and Nitrotetrazolium Blue ($NTBCl_2$) were commercially obtained from Fluka. Their formulae and abbreviations used in further text are listed in Figure 1.

The solvents employed such as acetonitrile (ACN), dimethylformamide (DMF), dimethylsulfoxide (DMSO) and methylene dichloride (MDC) were commercially obtained from Fluka. Electrochemical reduction was mainly carried out in an ACN solvent containing $2 \times 10^{-4}$ mol dm$^{-3}$ of substrate and $10^{-1}$ mol dm$^{-3}$ tetrabutylammonium perchlorate (TBAP) under an argon atmosphere. The cyclic

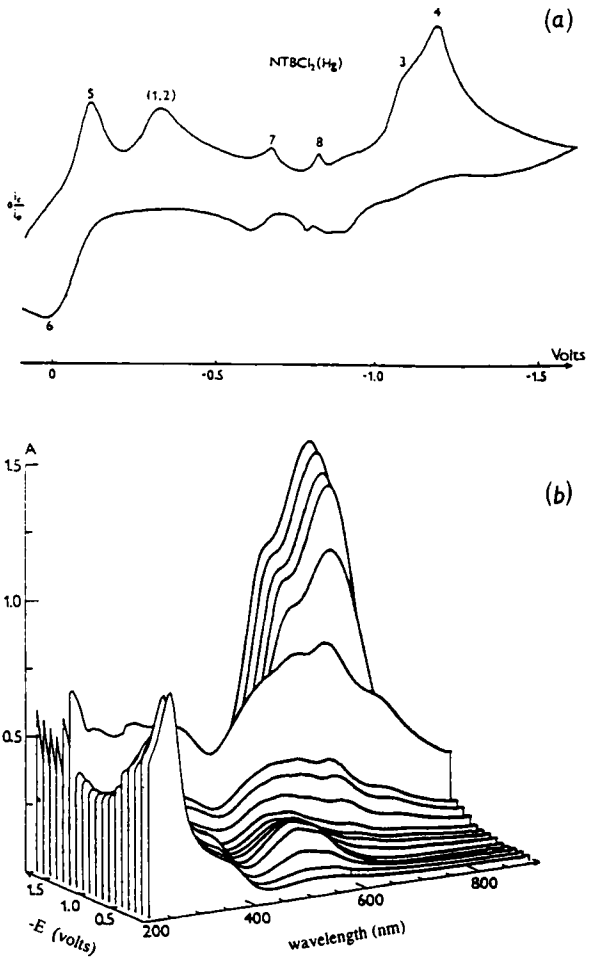


FIGURE 2 a) Cyclic voltammogram of $NTBCl_2$ cathodically reduced on the HMDE in ACN containing 0.1 M TBAP (scan rate 100 $mV.s^{-1}$).
Potentials are referred vs. SCE.
b) UV-VIS spectra observed during amperostatic reduction of $NTBCl_2$ at various potentials.

voltammetric experiments were performed with a PAR 270 system employing a three-electrode system with a platinum working electrode or hanging mercury drop electrode (HMDE), a platinum auxiliary electrode and a reference saturated calomel electrode (SCE) equipped with a Luggin capillary. *In-situ* electrochemical EPR experiments (SEEPR) were carried out in a Varian flat cell on a Bruker 200D spectrometer on line with an Aspect 2000 computer. EPR spectra were simulated employing Bruker standard programme.

In the flow spectra-electrochemical experiments, the EPR and UV flat cells were connected with an in house constructed electrolytic cell *via* membrane pump.[14] Working and counter platinum electrodes were separated by means of a fritted glass disk junction. UV-VIS spectra were recorded on Philips PU 8800 spectrometer.

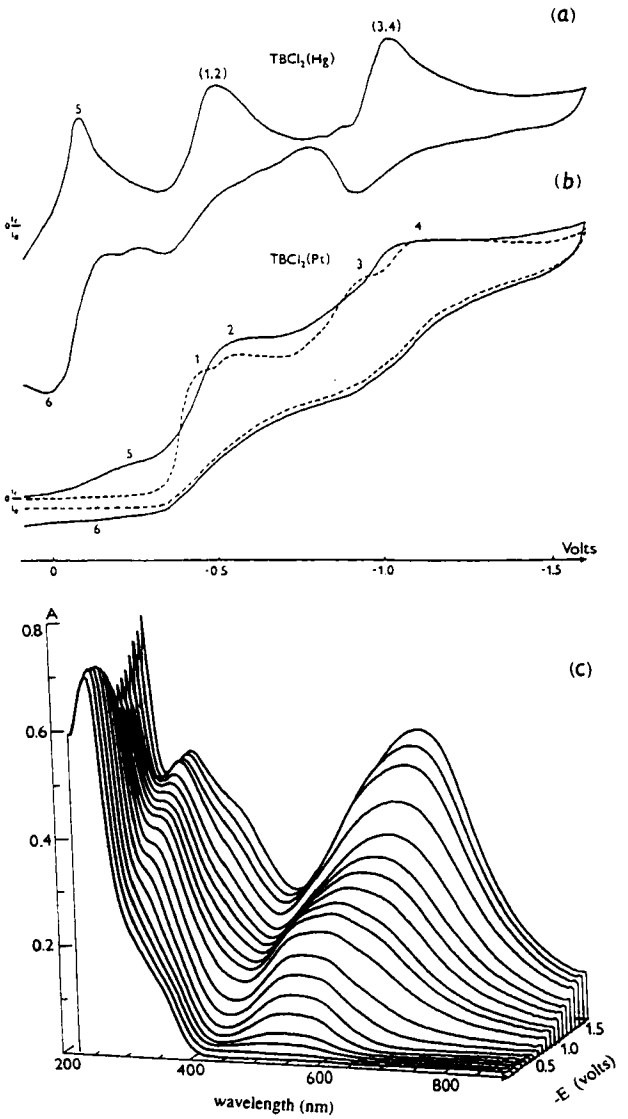


FIGURE 3 Cyclic voltammograms of $TBCl_2$ cathodically reduced on the HMDE (a) and platinum electrode (b) in ACN containing 0.1 M TBAP (scan rate 100 $mV.s^{-1}$). Potentials are referred vs. SCE. Further UV-VIS spectra observed during amperostatic reduction of $TBCl_2$ at various potentials (c).

## RESULTS AND DISCUSSION

### *Cyclic Voltammetry*

Figure 2a shows the cyclic voltammogram observed in the reduction of $NTBCl_2$ on the HMDE and Figure 3 in the reduction of $TBCl_2$ on the HMDE and platinum electrodes. Additionally, UV-VIS spectra obtained during amperostatic electrolysis

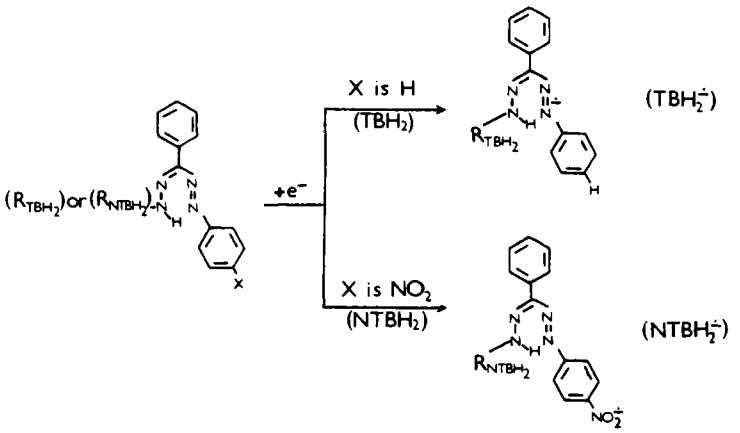


FIGURE 4 Reaction scheme of the reduction of formazans $TBH_2$ and $NTBH_2$.

of $NTBCl_2$ (Figure 2b) and $TBCl_2$ (Figure 3c) on the platinum gauze cathode are presented and will be discussed below. A characteristic feature of all voltammograms is two reduction peaks. The first one is in the region of $-0.3$ V for $NTBCl_2$ and $-0.5$ for $TBCl_2$ (with subpeaks 1,2) and the second one in the region of $-1.1$ V (with subpeaks 3,4). The character of these peaks indicates an adsorption and a diffusion process on the electrodes.[6] The second scan confirms this (dashed line in Figure 3b), where the peaks are clearly differentiated into the diffusion and the adsorption contribution.[6] At still lower potentials, (in the region of 0 V) further peaks (5,6) are observable. This is very pronounced on the mercury electrode (Figures 2a,3a) and less on the platinum electrode (Figure 3b). $TBCl_2$ and $NTBCl_2$ in contact with mercury and without polarisation give blue coloured solutions. This indicates the spontaneous reduction of $TBCl_2$ and $NTBCl_2$ to formazans. In Figure 3a, small peaks (7,8) are evident in the region from $-0.5$ to $-1$ V. They probably originate from the adsorption of the products formed in the initial stage of reduction. In the SEEPR experiments described below, radical products were found (Figure 5). Their EPR spectra are compatible with the formation of tetrazolinyl radicals (discussed later) according to the following reaction scheme:

$$K^{++} \xrightarrow{+e^-} K^{+\cdot} \xrightarrow{+e^-,\,RH} KH^+ \qquad (A)$$

$$KH^+ \xrightarrow{+e^-} KH\cdot \xrightarrow{+e^-,\,RH} KH_2 \qquad (B)$$

where K holds for TB and NTB. The radicals $K^{+\cdot}$ formed in (A) probably convert to diamagnetic products $KH^+$ abstracting hydrogen rapidly from the solvent. This explains the high degree of irreversibility found by the first reduction step. The H-abstraction from the solvent RH in (B) is probably slower and consequently, the $KH\cdot$ radical is observable. In the prolonged reduction formazans are formed and then reduced to the azo-type anion radical of $TBH_2$ and the nitro-centered anion radical of $NTBH_2$ according to the reaction scheme in Figure 4.

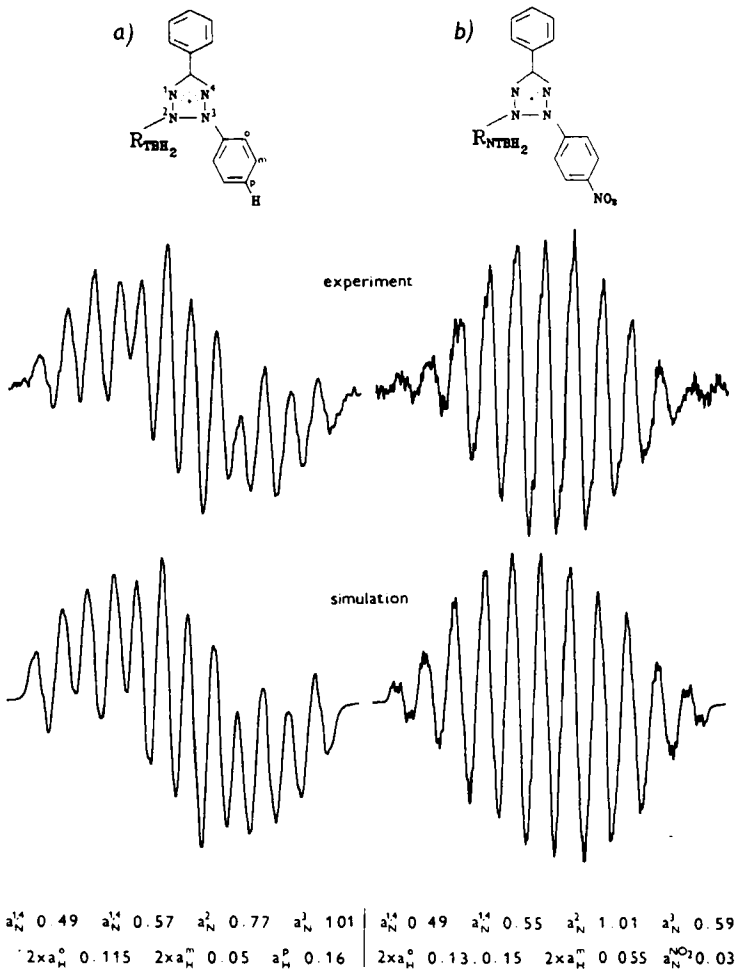


FIGURE 5 Experimental and simulated spectra of TBH· (a) and NTBH· (b) found in the cathodic reduction of $TBCl_2$ and $NTBCl_2$ at the potentials of the second reduction wave.

## *SEEPR Measurements*

***TBH· and NTBH·.*** $TBCl_2$ and $NTBCl_2$ were cathodically reduced directly in the cavity of EPR spectrometer. In the region of the first reduction wave, no radical products were observed. With ACN as the solvent, the radical intermediates found in the region of the second reduction wave are shown in Figure 5. Similar, but less resolved, spectra were obtained in the following aprotic solvents: DMF, DMSO, MDC. The spectrum of the TBH· radical (Figure 5a) was simulated assuming the interaction of unpaired electron with four non-equivalent nitrogen nuclei of the tetrazolyl ring with splitting constants $a_N^{1[4]} = 0.49\,mT$, $a_N^{4[1]} = 0.57\,mT$, $a_N^3 = 0.77\,mT$ and $a_N^2 = 1.01\,mT$. Figure 5 suggests the assignment of nitrogen splitting constants based on previous reports[11-13] where similar values for the

tetrazolyl skeleton were found. The further hyperfine structure of the individual lines (indicated but relatively poorly resolved) was satisfactorily simulated assuming the delocalisation of the unpaired electron on the phenyl ring in position 3 with splitting constants: $2xa_H^o = 0.115\,mT$, $2xa_H^m = 0.05\,mT$, $a_H^p = 0.16\,mT$. The g-value of the radical was 2.0040. Figure 5b shows the experimental and simulated spectra generated from nitroderivate of tetrazolium blue, i.e., NTBH· radical. Splitting constants $a_N^{1[4]} = 0.49\,mT$, $a_N^{4[1]} = 0.55\,mT$ and $a_N^2 = 1.01\,mT$ are similar to those found by the TBH· radical. In the case of NTBH· radical, the splitting constant $a_N^3 = 0.59\,mT$ decreased significantly when compared with $a_N^3 = 0.77\,mT$ in the case of TBH· radical and is in agreement with a similarly reported substitution effect.[11-13] This splitting constant was assigned to nitrogen in position 3. The splitting constants on the phenyl ring are: $2xa_H^o = 0.13$ and $0.15\,mT$, $2xa_H^m = 0.055\,mT$, $a_{NO_2}^p = 0.03\,mT$ while the g-value of the radical was 2.0040.

*$TBH_2^{-\cdot}$ and $NTBH_2^{-\cdot}$.* In the potential region over the second reduction wave, further radicals are formed. Figure 6a shows experimental and simulated spectra of radical generated from $TBH_2$. The splitting constants: $a_N = 0.59\,mT$, $a_N = 0.44\,mT$, $a_N = 0.26\,mT$, $2xa_H^m = 0.1\,mT$, $2xa_H^o = 0.31\,mT$ and $a_H^p = 0.35\,mT$ and $g = 2.0038$ suggest the anion radical of formazan $TBH_2^{-\cdot}$ with the center of unpaired electron on the azogroup nitrogens. Figure 6b shows experimental and simulated spectra of the radical generated from $NTBH_2$. The simulation extracted parameters: $a_N(NO_2) = 1.245\,mT$, $2xa_H^o = 0.34\,mT$ and $2xa_H^m = 0.11\,mT$, $a_N = 0.11\,mT$ and $a_N = 0.09\,mT$, $a_N = 0.02\,mT$ and $g = 2.0050$ indicate the anion radical $NTBH_2^{-\cdot}$ with the center of unpaired electron on the nitro group of $NTBH_2$. Additionally, after prolonged electrolysis, its cleavage product, the nitrobenzene anion radical, was observed.

### *UV-VIS Measurements*

The time-resolved UV-VIS spectra obtained for the amperostatic electrolysis of $TBCl_2$ and $NTBCl_2$ in ACN are presented in Figures 3c, 7, 2b, 8 respectively. Before electrolysis, both compounds exhibit absorption bands in the 230–260 nm region. At the beginning of the electrolysis and in the potential region of the first reduction wave, two new double bands in ranges 280–300 nm and 510–570 nm (violet) appeared and were observed to increase with electrolysis time. Simultaneously, the original 230–260 nm band decreased with an isosbestic point at 278 nm and 298 nm for $TBCl_2$ and $NTBCl_2$ respectively. No radical products were observed at this stage.

Increasing the potential in the region of the second reduction wave, the colour of electrolysed solutions changed from violet to blue and a new absorption band arose in the 550–580 nm range for $TBCl_2$ (*subfigure 7) with an isosbestic point at 644 nm, and a group of bands in the 350–900 nm range for $NTBCl_2$ (Figure 7c) *via* isosbestic point at 580 nm (Figure 7b). Simultaneously, EPR spectra of TBH· and NTBH· radicals shown in Figure 5 were found. The formation of blue coagulates (insoluble formazan) caused an increase of the baseline in UV-VIS spectra shown in Figure 8c.

Increasing the potential beyond the second reduction wave, the blue colour changed to light blue and an azo-type anion radical shown in Figure 6a was observed

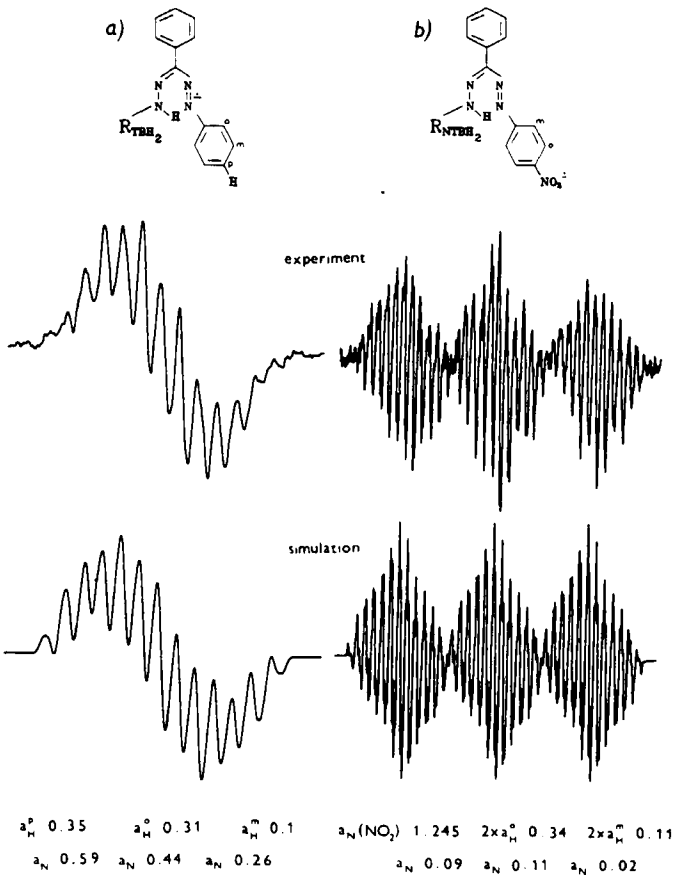


FIGURE 6 Experimental and simulated spectra of $TBH_2^{-\cdot}$ and $NTBH_2^{-\cdot}$ observed after prolonged reduction of their formazans $TBH_2$ and $NTBH_2$.

for $TBCl_2$. Analogously, a colour change from blue to green and the nitro group centered anion radical (Figure 6b) was observed for $NTBCl_2$. This corresponds well to the band observed in the 610–630 nm region for $TBCl_2$ (Figure 7) and with two bands at 450–470 nm and 680–730 nm (green) for $NTBCl_2$ with isosbestic points at 604 nm and 766 nm respectively (Figure 8d). The 680–730 nm band is still superimposable with previous spectra. It is noteworthy that during the amperostatic reduction, the conjugation in the $\pi$-electron systems of $TBCl_2$ and $NTBCl_2$ increases and results in colour changes from yellow to blue or green.

The redox-processes are reversible. That is, during electrolysis the obtained compounds can be electrochemically as well as aerobically oxidized step by step to the original compounds.

As in the UV-VIS measurements only superimposed spectra of the reduction products were obtained and were analysed using the Evolving Factor Analysis.[15] From the UV-VIS spectra set shown in Figure 2b ($NTBCl_2$) as well as in Figure 3c ($TBCl_2$) four compounds were identified and assigned to the following products: $TB^{+\cdot}$ ($\lambda_{max}^{calc.} = 250$ nm); $TBH^+$ ($\lambda_{max}^{calc.} = 237, 310, 525$ nm); $TBH_2$ ($\lambda_{max}^{calc.} = 557$ nm);

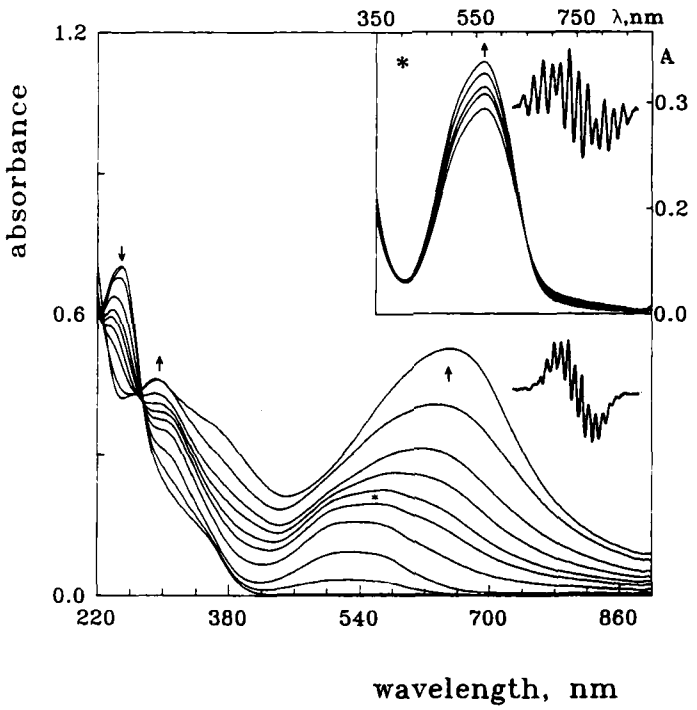


FIGURE 7 Time-resolved UV-VIS spectra observed during amperostatic reduction of $TBCl_2$ along with EPR spectrum of $TBH_2^{-\cdot}$ found at the end of electrolysis.
*subfigure 7 a more detail time resolution at the potential of the second reduction wave along with the EPR spectrum of there observed TBH· radical.

reduction products of $TBH_2$ ($\lambda_{max}^{calc.} = 660$ nm) for $TBCl_2$, and $NTB^{++}$ ($\lambda_{max}^{calc.} = 257$ nm); $NTBH^+$ ($\lambda_{max}^{calc.} = 257, 315, 517$ nm); $NTBH_2$ probably superimposed with spectrum of NTBH· ($\lambda_{max}^{calc.} = 365, 562, 610, 667, 770$ nm); reduction products of $NTBH_2$ ($\lambda_{max}^{calc.} = 460, 700$ nm) for $NTBCl_2$ respectively. Additionally analysis of *subfigure 7 implies the evidence of a further compound probably TBH· with $\lambda_{max}^{calc.} = 618$ nm.

## CONCLUSIONS

The electrochemical reduction of tetrazolium salts $TBCl_2$ and $NTBCl_2$ has been described so far in aqueous solutions with two 2-electron irreversible steps.[5,6] Because of rapid consecutive reactions no radical intermediates were identified. We expanded those studies to the non-protolytic solvents and additionally applied EPR and UV-VIS spectroscopy. The UV-VIS and electrochemical data obtained here are qualitatively similar to those found in aqueous solutions. However, the consecutive reactions are considerably slower and so it was possible to determine the individual reaction intermediates. The radical products formed in the potential range of the second reduction wave and also beyond these potentials were identified by means of EPR spectroscopy. The analogies between electrochemical and UV-VIS

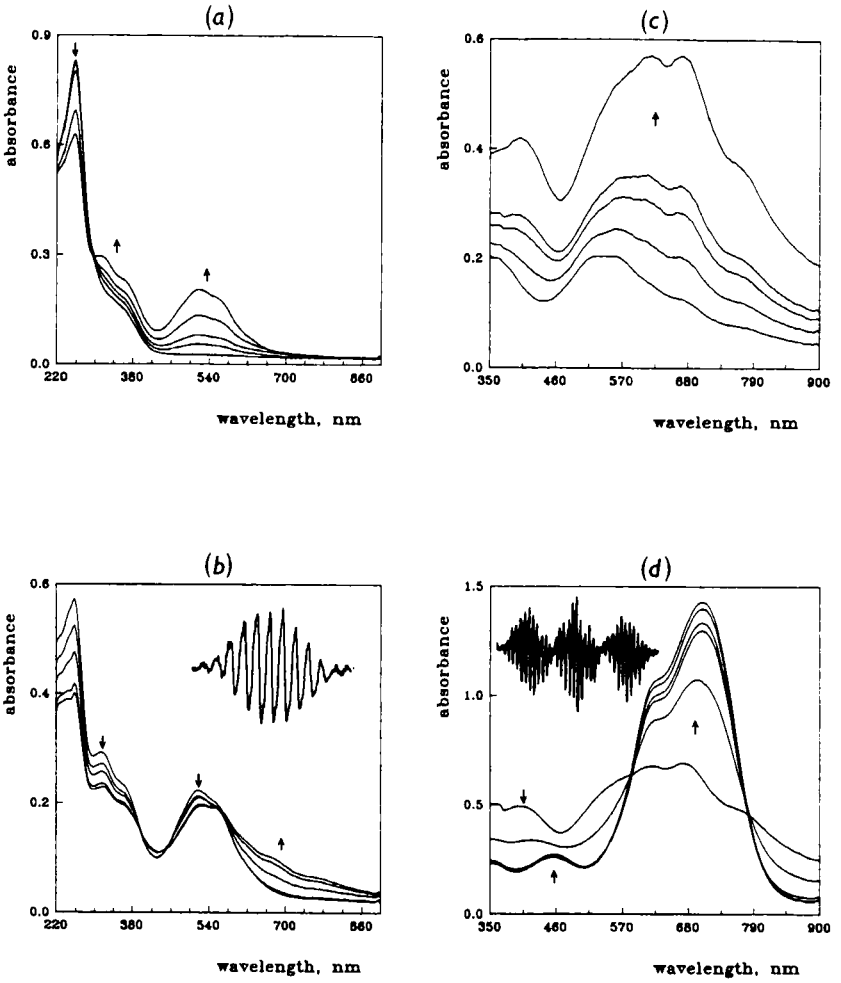


FIGURE 8 Time-resolved UV-VIS spectra observed during the amperostatic reduction of $NTBCl_2$ in the region of the first reduction wave (a), in the initial region of the second reduction wave along with the corresponding EPR spectrum of NTBH· radical (b), at the final region of the second reduction wave (c) and at the potential region beyond the second reduction wave along with the observed EPR spectrum of $NTBH_2^-$ (d).

data suggest similar reaction mechanism in aqueous and aprotic solvents. The results from electrochemical, UV-VIS and EPR measurements are summarised in Table 1.

## *References*

1. a) A.F. Jones, J.W. Winkles, P.J. Thornalley, P.E. Jennings and A.H. Barnett (1987) Inhibitory effect of superoxide dismutase on fructosamine assay. *Clinical Chemistry*, **33**, 147–149.
   b) C.J.F. Van Noorden (1988) On the role of oxygen in dehydrogenase reactions using tetrazolium salts. *Histochemical Journal*, **20**, 587–593.

TABLE 1
Summary of the results obtained from electrochemical, UV-VIS and EPR measurements.

**1st reduction wave**

| | ditetrazolium $K^{++}$ | | tetrazolinyl radical $K^{+\cdot}$ | | monoformazan $KH^{+}$ | | Note |
|---|---|---|---|---|---|---|---|
| | $TB^{++}$ | $NTB^{++}$ | $TB^{+\cdot}$ | $NTB^{+\cdot}$ | $TBH^{+}$ | $NTBH^{+}$ | |
| UV-VIS | 250 | 257 | not observed, short life time | | 237<br>310<br>525 | 257<br>315<br>517 | $\lambda_{max}^{calc.}$ in nm |
| Cyclic voltammetry | first reduction wave - irreversible<br>$K^{++} \xrightarrow{+e^-} K^{+\cdot} \xrightarrow{+e^-, RH} KH^{+}$ | | | | | | Potential region<br>~ -0.5 V for $TB^{++}$<br>~ -0.3 V for $NTB^{++}$ |
| EPR | radicals not observed | | | | | | |

**2nd reduction wave**

| | monoformazan $KH^{+}$ | | tetrazolinyl radical $KH\cdot$ | | formazan $KH_2$ | | Note |
|---|---|---|---|---|---|---|---|
| | $TBH^{+}$ | $NTBH^{+}$ | $TBH\cdot$ | $NTBH\cdot$ | $TBH_2$ | $NTBH_2$ | |
| UV-VIS | 237<br>310<br>525 | 257<br>315<br>517 | (618) | (356)<br>(562)<br>(610)<br>(770) | 660 | 365<br>562<br>610<br>770 | $\lambda_{max}^{calc.}$ in nm<br>$KH\cdot$ and $KH_2$ spectra are superimposed |
| Cyclic voltammetry | second reduction wave - reversible<br>$KH^{+} \xrightarrow{+e^-} KH\cdot \xrightarrow{+e^-, RH} KH_2$ | | | | | | Potential region<br>~ -1.1 V for $TBH^{+}$<br>~ -1.1 V for $NTBH^{+}$ |
| EPR | stable $TBH\cdot$ and $NTBH\cdot$ radicals | | | | | | after prolonged reduction $KH_2^{-}\cdot$ radicals observable |


c) C.J.F. Van Noorden and R.G. Butcher (1989) The involvement of superoxide anions it the nitro blue tetrazolium chloride reduction mediated by NADH and phenazine methosulfate. *Analytical Biochemistry*, **176**, 170–174.

2. P. Kivalo and K.K. Mustakallio (1956) A polarographic study of some tetrazolium compounds. *Suomen Kemi*, **298**, 154.
3. B. Jambor and E. Bajsuz (1956) Polarographic investigation of ditetrazolium salts. *Agrokemia Talajtan*, **5**, 117.
4. P.N. Gupta and A. Raina (1990) Electrochemical behaviour of blue tetrazolium in acid buffers. *Journal of the Indian Chemical Society*, **67**, 247–248.

5. M.I. Viseu, M.L.S.S. Goncalves, S.M.B. Costa and M.I. C. Ferreira (1990) Mechanism of the electrochemical reduction of tetrazolium blue in non-ionic micelles Part I. Polarography. *Journal of Electroanalytical Chemistry*, **282**, 201–214.
6. M.I. Viseu, M.L.S.S. Goncalves, S.M.B. Costa and M.I.C. Ferreira (1990) Mechanism of the electrochemical reduction of tetrazolium blue in non-ionic micelles Part II. Cyclic voltammetry and controlled-potential coulometry. *Journal of Electroanalytical Chemistry*, **282**, 215–227.
7. R.G. Butcher (1978) The measurement in tissue sections of the two formazans derived from nitroblue tetrazolium in dehydrogenase reactions. *Histochemical Journal*, **10**, 739–744.
8. R.G. Butcher and F.P. Altman (1973) Studies on the reduction of tetrazolium salts II. The Measurement of the half reduced and fully reduced formazans of neotetrazolium chloride in tissue sections. *Histochemie*, **37**, 351–363.
9. B.H.J. Bielski, G.G. Shine and S. Bajuk (1980) Reduction of nitro blue tetrazolium by $CO_2^-$ and $O_2^-$ radicals. *Journal of Physical Chemistry*, **84**, 830–833.
10. Y. Deguchi and Y. Takagi (1967) ESR spectrum of 2,3,5-triphenyl tetrazolium. *Tetrahedron Letters*, **33**, 3179–3180.
11. F.A. Neugebauer and G.A. Russell (1968) Tetrazolinyl radicals. *Journal of Organic Chemistry*, **33**, 2744–2746.
12. a) L.S. Podenko, A.K. Tchirkov and V.P. Schipanov (1980) ESR study of the electron structure of tetrazolinyl radicals. *Zhurnal Strukturnoi Khimii*, 161–163.
    b) L.S. Podenko, A.K. Tchirkov and V.P. Schipanov (1981) ESR study of the isotropic splitting constants of tetrazolinyl radicals. *Zhurnal Struktunoi Khimii*, 187–189.
13. N. Azuma, K. Mukai and K. Ishizu (1970) ESR studies of radicals generated by the $PbO_2$. Oxidation of some mono- and bis-formazans. *Bulletin of the Chemical Society of Japan*, **43**, 3960–3962.
14. P. Rapta (1993) Ph.D. Thesis, Slovak Technical University.
15. H. Gampp, M. Maeder, Ch. J. Meyer and A.D. Zuberbuhler (1986) Calculation of equilibrium constants from multiwavelength spectroscopic data - IV. *Talanta*, **33**, 943–951.

Accepted by Professor Dr. Hermann Esterbauer